Neuron, Vol. 19, 175–184, July, 1997, Copyright ©1997 by Cell Press

Gated Access to the Pore of a Voltage-Dependent K^+ Channel

Yi Liu,* Miguel Holmgren,* Mark E. Jurman, and Gary Yellen
Department of Neurobiology
Harvard Medical School
and Massachusetts General Hospital
Boston, MA 02114

Summary

Voltage-activated K^+ channels are integral membrane proteins that open or close a K^+-selective pore in response to changes in transmembrane voltage. Although the S4 region of these channels has been implicated as the voltage sensor, little is known about how opening and closing of the pore is accomplished. We explored the gating process by introducing cysteines at various positions thought to lie in or near the pore of the Shaker K^+ channel, and by testing their ability to be chemically modified. We found a series of positions in the S6 transmembrane region that react rapidly with water-soluble thiol reagents in the open state but not the closed state. An open-channel blocker can protect several of these cysteines, showing that they lie in the ion-conducting pore. At two of these sites, Cd^{2+} ions bind to the cysteines without affecting the energetics of gating; at a third site, Cd^{2+} binding holds the channel open. The results suggest that these channels open and close by the movement of an intracellular gate, distinct from the selectivity filter, that regulates access to the pore.

Introduction

Voltage-activated K^+ channels open and close a K^+-selective pore in response to changes in the transmembrane voltage. Understanding this gating mechanism involves answering two types of questions: how does the protein sense the change in voltage, and how does the pore then open and close? Recent studies on Na^+ and K^+ channels have provided evidence that movement of the charged S4 region plays a role in voltage sensing (Sigworth, 1994; Aggarwal and MacKinnon, 1996; Larsson et al., 1996; Seoh et al., 1996; Yang et al., 1996). Less is known about the molecular nature of the pore gating process. Does the selectivity filter constrict, does part of the pore collapse, or is there a separate trap door or gate that restricts access to the pore?

The best information about the gates of voltage-dependent K^+ channels has come from the pioneering work of Armstrong on the effects of intracellularly applied quaternary ammonium (QA) blockers (Armstrong, 1966, 1971, 1975). He found that tetraethylammonium and its long-chain derivatives could block the squid axon delayed rectifier K^+ channel, specifically when the channel activation gates were open. This was particularly apparent for high affinity long chain derivatives like nonyltriethylammonium (C_9), which made the delayed rectifier K^+ channels appear to inactivate. In the presence of C_9, the initial response to depolarization was a normal outward current, followed by a relaxation phase representing the blockade of open channels by C_9. Experiments like these led to the hypothesis that the intracellular mouth of the channel, containing the receptor for the QA compounds, could be exposed or hidden in response to voltage changes.

To learn more about pore gating at the molecular level, we have used site-directed mutagenesis to substitute cysteine at specific sites in the channel protein. These introduced cysteines were then chemically modified with methanethiosulfonate (MTS) reagents to test their reactivity. This general strategy has been used by many workers to learn about protein structure, in the absence of more direct methods (Falke et al., 1988; Akabas et al., 1992; Sahin Toth and Kaback, 1993). It has also been used to study changes in protein structure that occur during interesting conformational changes involved in signaling. The goal in this case is to introduce cysteines that do not interfere much with the signaling process of interest, and then to measure the state-dependent rate of chemical modification in different conformational states of the protein. This approach has been used for bacterial chemotaxis receptors (Chervitz and Falke, 1995). It has also been used to provide evidence for the movement of the S4 voltage-sensor in Na^+ and K^+ channels (Yang and Horn, 1995; Larsson et al., 1996; Yang et al., 1996) and for the movement of the outer mouth of the K^+ channel pore during C-type inactivation (Yellen et al., 1994; Liu et al., 1996).

The S6 transmembrane region (Figure 1) has been proposed as a candidate for the lining of the intracellular mouth of the voltage-dependent K^+ channel pore, based on the effects of mutations in this region on the binding of open channel blockers and on single channel conductance (Choi et al., 1993; Shieh and Kirsch, 1994; Lopez et al., 1994; Taglialatela et al., 1994). Also, genetic selection for gating dysfunction from random mutants of a yeast K^+ channel has yielded mutations in the S6 region with altered gating (Loukin et al., 1997). We introduced cysteines in this region as targets for chemical modification by MTS reagents. We found that for many of these introduced cysteines, the rate of chemical modification was extremely dependent on whether the channel was open or closed. To learn more about where these cysteines sit in relationship to the pore and its gate, we have also studied the ability of open channel blockers to protect the cysteines from reaction, and the ability of Cd^{2+} ions to bind to the cysteines and modify gating. Our results support the idea that there is an activation gate on the intracellular end of the pore, distinct from the selectivity filter, that regulates communication between the intracellular bathing solution and the pore-lining part of S6.

*These authors contributed equally to this work.

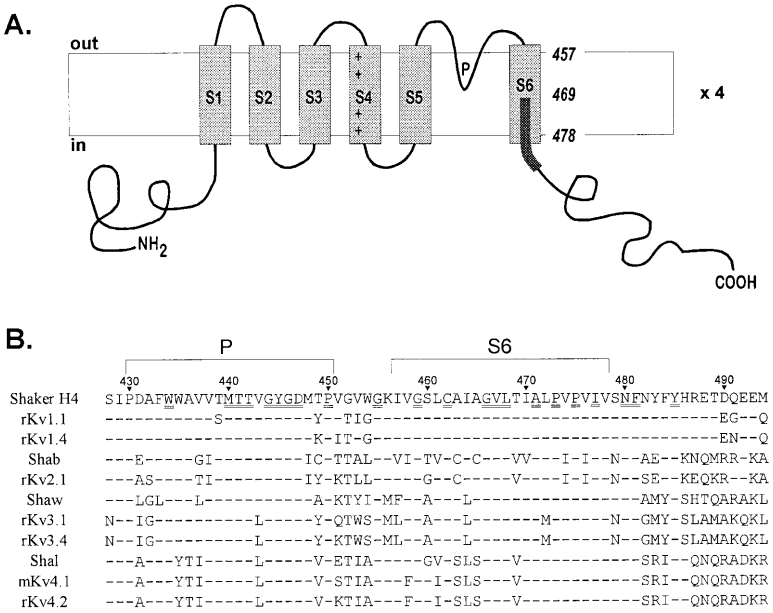

Figure 1. Schematic of K^+ Channel Subunit Structure and the S6 Transmembrane Segment

(A) Transmembrane folding model for a subunit of a homotetrameric Shaker K^+ channel, with residue numbering in S6. The nominal limits of S6 from hydrophobicity analysis (Tempel et al., 1987) extend roughly from residues 457 to 478, though the region of strong evolutionary conservation extends somewhat further (to about 485). We focused on the region indicated by the thickened line (from 469–486).

(B) Amino acid sequence from related K^+ channels of different families, showing the amino acid conservation in the P and S6 regions. Dashes indicate residues that are the same as the corresponding Shaker H4 residue. Underscored residues are completely conserved in the Kv1.x-Kv4.x family. The numbering is that for the Shaker K^+ channel.

Results

State-Dependent Reactivity of Cysteines Introduced in S6

An example of a cysteine mutant in the S6 region with state-dependent reactivity to intracellular thiol reagents is shown in Figure 2A. The 474C mutant channels in this inside-out patch were held closed at a voltage of −90 mV, and their activity was monitored using brief activating pulses to 0 mV every 4 s. The channels were first treated in the closed state for 5 s with 100 μM trimethylaminoethyl-MTS (MTSET), and there was no change in the current amplitude. By contrast, when the channels were treated for 100 ms in the open state with the same concentration of MTSET, current amplitude was irreversibly reduced by ~85%. This shows that the introduced cysteine at 474 is much more reactive to intracellularly applied reagents when the channel is open.

To confirm that this large change in reactivity was related to channel gating rather than to some other effect

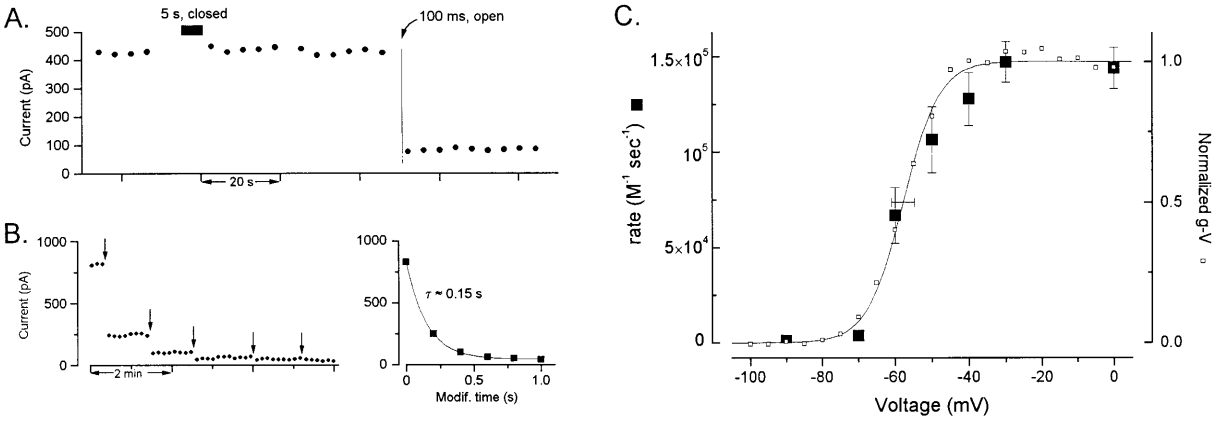

Figure 2. Gating State Dependence for Chemical Modification of an S6 Cysteine

(A) Chemical modification of channels with a cysteine at position 474. Voltage clamp current was measured from an inside-out patch containing 474C channels. From a holding potential of −90 mV, brief test pulses (10 ms) to 0 mV were applied to measure the current through the channels (closed circles). MTSET (100 μM) was applied for 5 s to closed channels, with no effect. Applying the same concentration of MTSET for 100 ms with the channels open (during a 140 ms pulse to 0 mV) reduced the current by ~85%.

(B) Typical measurement of the modification rate constant. Left: dots indicate the steady-state current in response to brief pulses to 0 mV; every other pulse is shown. Arrows indicate times at which 100 μM MTSET was applied for 200 ms, during a voltage step to −60 mV. Right: remaining current as a function of cumulative modification time. The reciprocal of the time constant is divided by the [MTSET] to give a second-order rate constant of ~67,000 M^{-1} s^{-1}.

(C) Voltage dependence of the MTSET modification rate of 474C channels (closed squares). For comparison, normalized g–V data obtained from tail currents is shown (open circles). The solid line is a Boltzmann function with slope and midpoint equal to the mean values for independent fits to four experiments; the horizontal error bar shows the standard deviation of the midpoint.

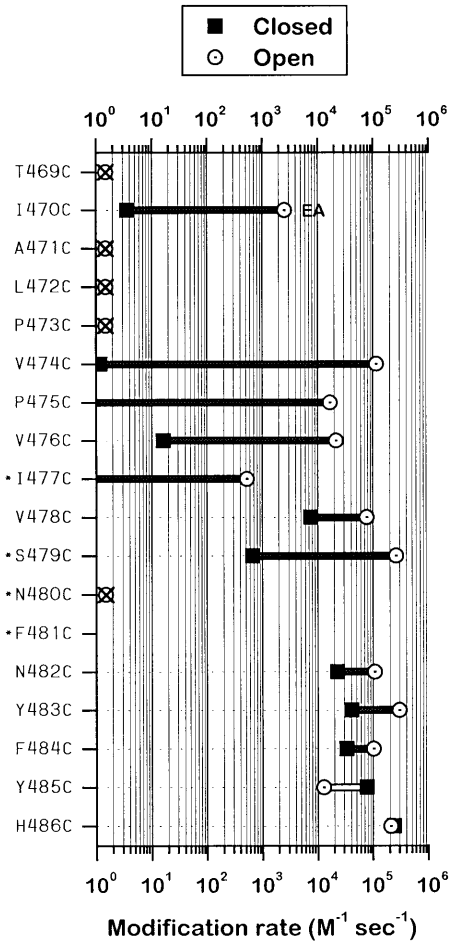

Figure 3. State-dependent Accessibility of S6 Cysteine Mutants

Second-order rate constants are plotted for cysteine modification in the closed (closed squares) and open (open circles) states. On this logarithmic scale, the length of the bar connecting the two symbols gives the fold-change in rate between the open and closed states (closed bar for $k_{Open} > k_{Closed}$, open bar for $k_{Closed} > k_{Open}$). Positions marked with ⊗ were not substantially affected by MTSET or MTSEA treatment, compared with control "wild-type" channels. MTS reagents were applied from the intracellular side. MTSET was used for all positions except 470; for this mutant, MTSEA but not MTSET produced a change in current. Modification at most positions was monitored by the reduction of current; at position 476 we measured the fraction of current with altered gating (see Figure 7), and at positions 483 and 486 we measured the loss of Cd^{2+} sensitivity. Mutants marked with an asterisk (*) were studied as tandem dimers, with only one of the two protomers containing the mutation (these mutants did not express functionally as homotetramers); the F481C mutant did not express even as a tandem dimer. Closed state modification at positions 475 and 477 was slower than 1 M^{-1} s^{-1}. Each point is the mean of three or more determinations; standard errors are all smaller than the symbols.

of voltage (such as the movement of the reagent into the membrane field), we studied the detailed voltage dependence of the reactivity. The reaction rate was obtained by measuring the time course of current reduction upon repeated brief applications of MTSET (Figure 2B), and the rate of the single exponential time course was used to compute a second-order reaction rate constant. Figure 2C shows that the reaction rate rose steeply with depolarization, in parallel with the channel gating (g–V) curve, and it reached a plateau value at voltages giving the maximum open probability. This result is consistent with gated access of the reagent to the cysteine. The maximum reaction rate constant of ~144,000 M^{-1} s^{-1} is very large and comparable to the rate constant for MTSET reaction with free mercaptoethanol (~90,000 M^{-1} s^{-1}; from Stauffer and Karlin, 1994).

This approach was applied systematically to determine the state-dependent reactivity of cysteines introduced at positions 469 through 486, one at a time. The cysteine mutant channels generally had little alteration in their gating. Almost all of the channels had a midpoint voltage for activation in the range −70 mV to −35 mV, and a 20%–80% risetime (at 0 mV) in the range of 0.5–1.5 ms. The two exceptions were for the two proline-to-cysteine mutations: P473C had slow activation kinetics (~3 ms risetime at 0 mV), and P475C had a large shift in voltage dependence (midpoint ~5 mV) and very slow activation kinetics (~30 ms at 40 mV). One mutant in this region (F481C) did not give functional expression in homotetramers or in a dimer with one mutant protomer; transfection with a mixture of mutant and wild-type expression plasmids gave currents that could not be distinguished from wild type.

Figure 3 shows the pattern of state-dependent reactivity of cysteines substituted in S6. For each mutant studied, we measured the apparent second-order reaction rate constant in the closed and open states. The values for closed and open state rates are plotted on a logarithmic axis, so that the length of the bar connecting them shows the fold-change in cysteine reactivity between the two states. The deepest accessible cysteines, at positions 470 and 474–477, showed modification almost exclusively in the open state, with a 400- to 50,000-fold slower rate of modification in the closed state. Residues located further toward the C-terminus (and outside the traditional confines of S6; positions 482–486) showed much smaller changes in reactivity with gating, with a ≤10-fold preference either for the open or for the closed state.

This overall pattern leads us to hypothesize that access of MTS reagents to the deeper region (470–477) is controlled by the activation gate of the channel, much as access of K^+ ions to the pore is regulated. In the lower S6 and beyond (482–486), we suppose that access is not gated but that there is gating-associated movement that results in significant but smaller changes in side-chain accessibility or environment. Similar 5- to 10-fold changes in cysteine reactivity with gating have been seen in the S4–S5 linker region (Holmgren et al., 1996a).

Protection of S6 Cysteines by an Open-Channel Blocker

The idea that access to the deeper S6 cysteines is regulated by the activation gate assumes that these residues lie within the central ion-conducting pore of the channel. To test this assumption, we measured the ability of a known open-channel blocker, tetrabutylammonium (TBuA; French and Shoukimas, 1981), to protect cysteines at the two deepest positions (470 and 474) from reaction with the MTS reagents. For example, when the

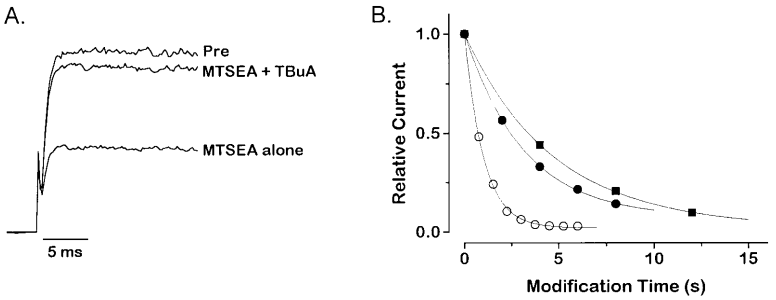

Figure 4. An Open-Channel Blocker Protects the Cysteine at 470C

(A) Outward current through 470C mutant channels, before MTSEA treatment, after treatment in the presence of TBuA, and after treatment without blocker. Data from an inside-out patch with depolarization from −90 to +60 mV; the pretreatment current level was 400 pA. In the presence of 100 μM TBuA (yielding ~90% steady-state blockade), treatment with 400 μM MTSEA for 0.75 s produced only a small amount of current reduction. In the same patch, a similar treatment with no blocker resulted in substantial current reduction.

(B) Modification time course, without blocker (open circles; $\tau \approx 1.0$ s), with 64% blockade (filled circles; $\tau \approx 3.2$ s), or with 80% blockade (open squares; $\tau \approx 4.7$ s). If TBuA protects the cysteines completely, these amounts of blockade are predicted to slow the modification rate by 2.7- and 4.9-fold, respectively.

470C mutant was treated with MTSEA in the presence of 100 μM TBuA, there was very little modification compared with the same treatment in the absence of blocker (Figure 4A). Using different concentrations of TBuA to vary the fractional blockade, we found that the degree of protection was well-correlated with the degree of blockade (Figure 4B). For instance, when channels were ~80% blocked, the modification rate was ~4.7-fold slower than the control, compared with the predicted value of ~5-fold slower if blocked channels were completely protected from modification. This indicates that the protection effect is likely to be caused by TBuA acting at its block site. Similar results were obtained for the 474C mutant (data not shown), consistent with these positions lying in the pore, behind or near the binding site for TBuA.

Energetics of Gating When Cd^{2+} Is Bound to the Introduced Cysteines

We also used Cd^{2+} ions as a probe to learn how some of the introduced cysteines might move during gating. Because of the tight interaction between Cd^{2+} and the thiol side chains of cysteine, Cd^{2+} ions have strong and specific effects on some of the mutant channels. We studied several of the deep region mutants to see how Cd^{2+} binding interacted with gating.

For example, the mutant 474C was inhibited by Cd^{2+} with very high affinity. There was little inhibition when the channels were held closed at a negative voltage, but inhibition occurred rapidly when the channels were open (Figure 5A), just as for the MTS reagents. This Cd^{2+} inhibition was essentially irreversible, even in the presence of the chelator EGTA. However, Cd^{2+} could be released from the channel by the di-thiol compound 2,3-dimercapto−1-propanesulfonate (DMPS), particularly during a long depolarizing pulse (Figure 5A).

The extremely tight binding of Cd^{2+} to the 474C mutant suggests that the metal ion may interact with several of the four cysteines at this position in the homotetramer. DMPS probably releases Cd^{2+} from this tight binding site by using its two vicinal thiols to displace the protein ligands (Figure 5B), much as it releases arsenical reagents from multi-cysteine binding sites (Loring et al., 1992; Liu et al., 1996). To test whether Cd^{2+} binds to multiple 474 cysteines, we studied a channel having only two instead of four cysteines at this position, by expressing tandem dimers with a 474C mutation only in the first protomer. Unlike the homotetramer, these channels show spontaneous dissociation of bound Cd^{2+} ($\tau_{off} = 0.9 \pm 0.1$ s for dimers versus $\tau > 10$ min for homotetramers, both at 0 mV). This strong dependence of Cd^{2+} affinity on the number of cysteines argues that the Cd^{2+} interacts with multiple 474 cysteines; it also supports the conclusion that these cysteines line the pore and are near its axis.

Does this tight interaction of a Cd^{2+} ion with multiple 474 cysteines in different subunits affect the ability of the channel protein to go through the motions of gating? If these cysteines move substantially during gating, then the bridging of these cysteines by a Cd^{2+} should introduce a strong energetic bias in favor of either the open or the closed state—whichever state is closest to the optimum position for Cd^{2+} binding.

We were able to learn about the energetics for channel gating while Cd^{2+} was bound to 474C by measuring the voltage dependence of Cd^{2+} release. The rate of Cd^{2+} release in the presence of a fixed concentration of DMPS was measured at a series of different voltages (Figure 5C). This voltage dependence was very steep and tended to saturate, much like the Boltzmann function that is used to describe channel gating. This voltage dependence is consistent with the hypothesis that channels can open and close while Cd^{2+} is bound, and only when the channels are open can the Cd^{2+} be released by intracellular DMPS (Figure 5D). The apparent release rate, β_{app}, should then be a function of the probability that the channel gate is open, given that the channel is blocked, P(O | B):

$$\beta_{app} = \beta \cdot P(O \mid B)$$
$$= \beta \cdot P(OB)/[P(CB) + P(OB)]$$

where β is the maximal release rate from the open state (β is also proportional to [DMPS]).

In spite of the very strong binding of Cd^{2+}, which involves cysteines in multiple subunits, the voltage dependence for gating in the presence of Cd^{2+} (determined from β_{app}) was virtually unaltered from that of 474C channels in the absence of Cd^{2+} (Figure 5C). This is consistent with the idea that the amino acid residues at position 474 do not move much during gating. We consider this in more detail in the Discussion.

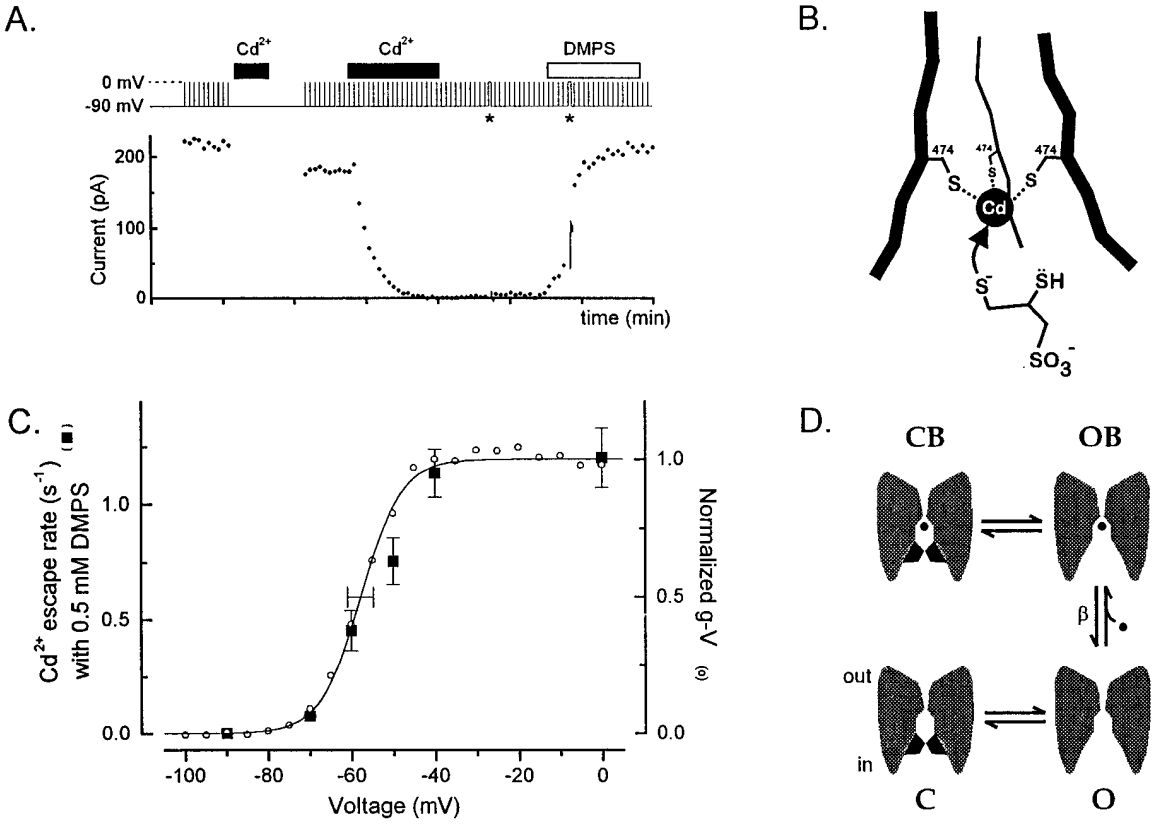

Figure 5. Cd^{2+} Bound to the 474C Mutant Is Trapped by Channel Closing, but It Produces Little Change in Gating

(A) Cd^{2+} interaction with 474C channels. Dots show the steady-state current level during 10 ms depolarizations from −90 to 0 mV. Cd^{2+} application (20 μM) to closed channels produced little inhibition, but application during a series of depolarizing pulses producing complete inhibition was not reversed by removing Cd^{2+} and washing with EGTA. Cd^{2+} could be removed only by applying the di-thiol DMPS (0.1 mM) at relatively positive voltages. The *'s indicate 2 s depolarizing pulses.

(B) A cartoon showing the hypothesized interaction of the bound Cd^{2+} with several 474 cysteines from different subunits. One subunit of the homotetramer is cut away. The di-thiol DMPS can release the bound Cd^{2+}, presumably by displacing the protein groups binding to the Cd^{2+} ion.

(C) Voltage dependence of Cd^{2+} escape from 474C, in the presence of 0.5 mM DMPS. Escape rates (closed squares) are compared with normalized g–V measurements (open circles) for the 474C channels, shown as in Figure 2C. There is <0.5 kcal/mol difference between Cd^{2+}-blocked and unblocked channels in the equilibrium constant for gating.

(D) Schematic for Cd^{2+} trapping. Cd^{2+} ions can enter the channels from the intracellular side only in the open state; once it enters, channels can reclose (to the CB state), preventing Cd^{2+} from being released by DMPS. Measurements of the Cd^{2+} escape rate (C) report the CB ⇌ OB equilibrium, while g–V measurements report the C ⇌ O equilibrium.

A similar phenomenon occurs at the 470 site. DMPS is again required for rapid release of Cd^{2+} from the 470C mutant, although there is a measurable rate of spontaneous Cd^{2+} release from this mutant (0.016 ± 0.002 sec^{-1} at 0 mV). The voltage dependence of release is again similar to the voltage dependence of normal (unblocked) channel gating (Figure 6), though opening of Cd^{2+}-blocked channels occurred at slightly more negative voltages. This shift corresponds to a rather small change of ⩽ 1 kcal/mol in the energetics of gating, with Cd^{2+} binding favoring the open state.

Cd^{2+} Binding to a Cysteine at 476 Holds the Channel Open

At the nearby 476 position, the effect of Cd^{2+} was quite different: Cd^{2+} bound to 476C channels held them open. This effect was relatively easy to see, because Cd^{2+} did not prevent current flow through the pore. Figure 7A shows the effect of 20 μM Cd^{2+}, in the presence of 50 mM extracellular K^+ to make the inward currents more prominent. After Cd^{2+} was applied, the channels remained open even upon repolarization to −110 mV (Figure 7A, 1), and they carried a constant inward current. A subsequent depolarization (Figure 7B, 2) produced only an instantaneous change in the direction and amplitude of current through the channels, with no time-dependent gating (Figures 7A and 7B, trace b). This inward current at −110 mV did decay very slowly, but this decay was apparently due to inactivation of the open channels, since outward current evoked after this decay (Figure 7A, 3) was also smaller and was still instantaneous. At the very negative voltage of −160 mV, the channels did close slowly in the presence of Cd^{2+} (with a time constant of 2.1 s). This closing most likely occurred by expulsion of Cd^{2+} from the channels, since a subsequent depolarization in the continued presence of

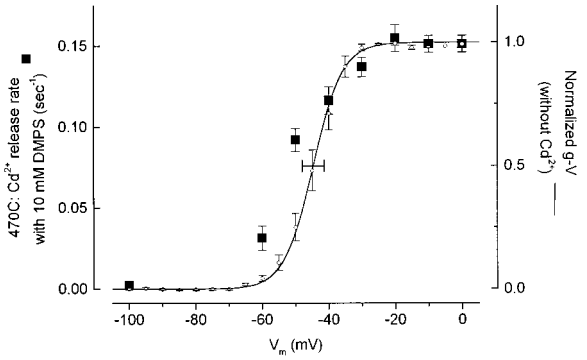

Figure 6. Gating of 470C Channels with a Bound Cd^{2+} Ion

Voltage dependence of the Cd^{2+} release rate from 470C channels is plotted. Cd^{2+} could not escape at negative voltages, but more positive voltages opened the channels and permitted release by 10 mM DMPS. The voltage dependence thus reflected the gating of Cd^{2+} blocked channels. For comparison, normalized g–V data are shown for 470C channels without Cd^{2+}; the horizontal error bar gives the standard deviation for the midpoint of the g–V curve.

Cd^{2+} opened the channels with kinetics just like those seen in the absence of Cd^{2+} (Figure 7A, 4; compare traces a and c in Figure 7B). Modification of 476C channels with MTS reagents also held them open without preventing current flow (data not shown).

Although we do not yet understand all of the features of these effects (for instance, the 20%–30% increase in the initial response with Cd^{2+}), they provide a clear contrast to the results with 470C and 474C, suggesting that the cysteine at 476 does participate somehow in gating. Also, unlike the other two mutants, the 476 position may not lie in the pore, since its reaction with MTSET is not prevented by blockade with TBuA (data not shown).

Discussion

S6 contributes to the pore lining

Our data strongly support the idea that part of S6 lines the gated intracellular part of the pore, which leads to the narrower ion-selective part of the pore formed by the P loop (Figure 8A, left). Several pieces of evidence suggest that the cysteines introduced at 470 and 474 contribute to the pore lining.

First, the cysteines at these sites were protected from MTS reaction by an open channel blocker, TBuA. An open channel blocker could, in principle, protect these sites by either a direct or indirect action. That is, it could interfere directly with reagent access to these sites, or it could induce a conformational change in the channel protein that makes these sites unreactive. There are two known ways in which open channel blockers like TBuA can alter the gating state of the channel: they can hold the activation gates open (Armstrong, 1971; French and Shoukimas, 1981; Choi et al., 1993), or they can affect C-type inactivation (Baukrowitz and Yellen, 1996a, 1996b). Neither of these effects is likely to be responsible for the protection effect. If the primary effect of TBuA were to hold the channel open, this would produce an increase in the reaction rate at these three sites, rather than the observed decrease. Also, we did all of the protection experiments using brief depolarizations and high external $[K^+]$, which should minimize C-type inactivation and any effects of the blockers on it. Therefore, although we cannot rule out some other type of allosteric interaction, it seems reasonable to interpret these protection effects as a direct blocker protection of cysteines in the pore.

Second, cysteines at position 474 in different subunits can apparently contribute to a single high-affinity binding site for Cd^{2+}. Spontaneous release of Cd^{2+} from the 474C mutant is not observed (in minutes) when four cysteines are present, but does occur when only two 474

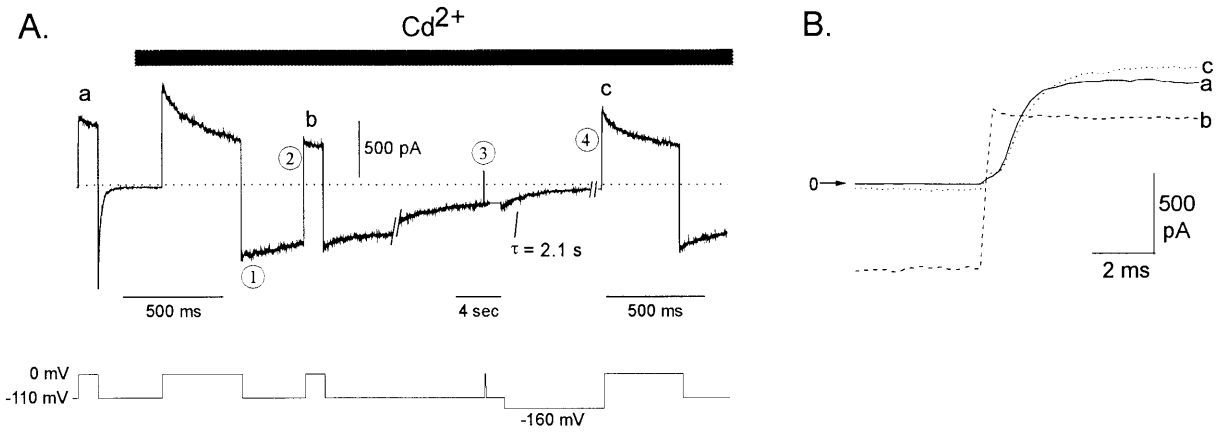

Figure 7. Cd^{2+} Binding to Cysteines at 476 Holds Channels Open

(A) Cd^{2+} (20 μM) was applied to an inside-out patch beginning 100 ms before the second of three depolarizing pulses to 0 mV. The channels failed to close completely after the 2nd pulse (1). There was some reduction in current at −110 mV after many seconds (slower time scale; center section), probably reflecting inactivation; significant closure occured at −160 mV, with a time constant of 2.1 s. A subsequent depolarization (faster time scale; 4) re-opens channels, which again fail to close completely at −110 mV.

(B) Expanded view of the rising phase of three pulses marked in (A). Trace b shows the instantaneous change in current of Cd^{2+}-treated channels, with no remaining time-dependent gating. Traces a (control) and c (in Cd^{2+}, after recovery at −160 mV) show a similar activation time course.

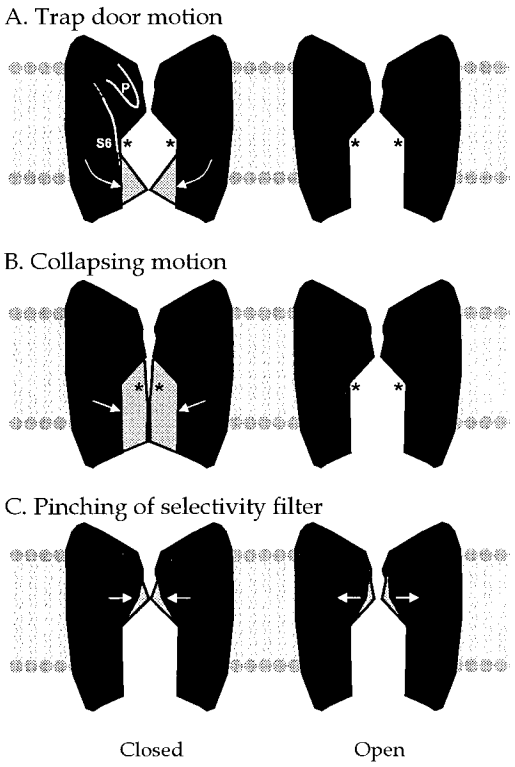

Figure 8. Three Models for K^+ Channel Activation Gating

(A) Intracellular gate. Between the gate and the selectivity filter is a cavity. In some K^+ channels this cavity can contain and trap organic blockers (Armstrong, 1971; Holmgren et al., 1997). Hypothetical positions are shown for the P loop (forming the selectivity filter) and the S6 (part of which lines the pore). Evidence that the P loop forms the selective part of the pore comes from mutagenesis studies (MacKinnon and Yellen, 1990; Yool and Schwarz, 1991; Hartmann et al., 1991; Yellen et al., 1991; Heginbotham et al., 1994).

(B) Collapse of the intracellular mouth. In (A) and (B), the asterisks (*) indicate the putative location of 470 and 474.

(C) Pinching-shut of the P-region selectivity filter (as proposed by Sun et al., 1996, for cyclic nucleotide gated channels).

cysteines are present. This argues that the 474 cysteines are close together near the axis of the channel, and therefore they probably line the pore.

Do the 470C and 474C Cysteines Remain Stationary during Gating?

Access to these pore-lining cysteines from the intracellular solution is controlled by activation gating. This could happen either because the cysteines move during the gating process (Figure 8B) or because access to the cysteines is regulated by a gate at the intracellular entryway to the pore (Figure 8A). We attempted to distinguish these possibilities by measuring the effect of Cd^{2+} binding on gating for the 470C and 474C mutants. We found that in spite of the strong interaction of Cd^{2+} with the cysteines at these positions, the inferred gating in the presence of Cd^{2+} had approximately the same voltage dependence as the gating in the absence of Cd^{2+}.

For a two-state model of gating, involving a voltage-dependent transition between the closed and open states, the absence of a shift can be interpreted in only one way: Cd^{2+} binds equally well to both states. In the diagram, the vertical arrows indicate the large favorable energy of Cd^{2+} binding.

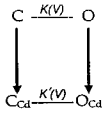

This conclusion would place tight constraints on the nature of the gating motion, since these cysteines could not move much (relative to each other) without affecting their interaction with Cd^{2+}. If the cysteines moved closer or further apart during gating, they would have different interaction energies in the open and closed states, and therefore Cd^{2+} would shift the gating curve. One could imagine that the lack of effect simply involves a cancellation of a favorable and an unfavorable effect of Cd^{2+}, but similar results are seen for Zn^{2+} release from the 474C mutant (data not shown), so this is unlikely. Overall, this analysis suggests that the amino acid residues at positions 470 and 474 line a part of the pore that remains static during gating, and that the strongly state-dependent reactivity of cysteines at these positions is due to a gate located between them and the intracellular solution (Figure 8A).

For a slightly more realistic three-state model of gating, the interpretation is less clearcut. We consider a model with two closed states, D and A. In this model, most of the voltage dependence is in the D ⇌ A equilibrium constant, and this represents the moving of the voltage sensor. The gate can then open in the A to O transition, which has little or no voltage dependence (Bezanilla et al., 1994; Zagotta et al., 1994). Using this basic scheme for gating in the absence of Cd^{2+}, there are three classes of models in which Cd^{2+} binding induces no shift in the apparent voltage dependence. In the following diagrams of these models, the top row is the gating in the absence of Cd^{2+}, and the vertical position denotes relative free energy:

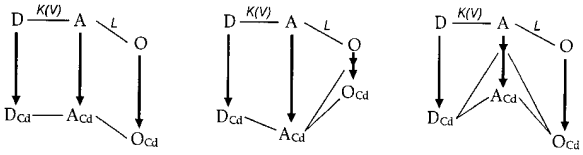

The first model is the simplest: there is no shift involtage dependence because Cd^{2+} binds all the states equally well. The second is quite different: it supposes that both the D and A states bind Cd^{2+} well, but the O state does not. This model works even if we assume that Cd^{2+} can be released only from the O_{Cd} state. Occupancy of the O_{Cd} state is very low, but it is always proportional to the occupancy of the A state, and its voltage dependence is much like the original voltage dependence of the O state. The slight preference of Cd^{2+} for the A state provides a small shift to compensate for the "loss" of the O state, which in the absence of Cd^{2+} tends to pull the equilibrium toward the right-hand states. The third class of models assumes equal Cd^{2+} binding to the D and O states, and is thus much like the first class. The only difference is that the intermediate A state is more or less disfavored when Cd^{2+} is bound, which affects the kinetics but not the D ⇌ O equilibrium.

Physically, the first two models are very different. In the first, neither movement of the voltage-sensor nor movement of the gate changes the Cd^{2+} binding energy, and the cysteines that interact with the Cd^{2+} do not move much during the entire gating process (as we concluded for the two-state model; Figure 8A). In the second model, the activation (voltage-sensor) step has little effect on Cd^{2+} binding, but the opening of the gate makes Cd^{2+} binding much worse. This could occur, for instance, if the cysteines pull apart in the O state but collapse around the Cd^{2+} in the D and A states (Figure 8B).

In both of these models, the fully-closed D state is capable of a strong favorable interaction with Cd^{2+}. (If it were not, the release of Cd^{2+} could not have a voltage dependence resembling that of gating, since the dominant voltage-dependent energy difference is between the D state and the other two.) In spite of this strong energetic interaction, the D state is kinetically inaccessible to Cd^{2+}; i.e., Cd^{2+} cannot enter the channels at negative voltages. We conclude that the failure of Cd^{2+} to inhibit the channels at negative voltages is due not to the absence of a high affinity Cd^{2+} site, but rather to gating-controlled access to this site.

Nature of the Gate

Our results are compatible either with an intracellular lid that covers the pore (Figure 8A) or with a collapse of the intracellular entryway to the pore (Figure 8B). They argue against the idea that the P region is the sole site of activation gating (Figure 8C), as proposed for cyclic-nucleotide-gated channels (Sun et al., 1996). However, we cannot exclude the possibility that both an intracellular gate and an extracellular gate (perhaps in the P region) move during activation gating (as suggested by Miller et al., 1987; Grissmer and Cahalan, 1989; but see Armstrong et al., 1982).

A separate line of evidence favors the idea of an intracellular lid, with a relatively static cavity located between this gate and the selectivity filter (Figure 8A). Large quaternary ammonium (QA) blockers of 8–10 Å in diameter can be trapped behind the activation gates in K^+ channels of the squid axon (Armstrong, 1971) and the node of Ranvier (Armstrong and Hille, 1972). This effect is not seen for wild-type Shaker K^+ channels, but it can be observed in Shaker 470C mutant channels, which trap organic blockers very efficiently (Holmgren et al., 1997). The blockers TEA and decyltriethylammonium can be trapped in these channels, and the gating of blocker-occupied channels is shifted by only ~10 mV. Channels close around a blocker with no additional effort, favoring the idea that in the closed state there is a substantial cavity lying behind the activation gate, rather than a complete collapse of the pore.

The gated pore of these channels thus appears to be a special instance of an enzyme active site that can be covered by a gate, possibly a hinged lid like that seen in structural studies of other types of natural and engineered proteins (for examples, see Joseph et al., 1990; Fitzgerald et al., 1996). The precise identity and motion of the intracellular activation gate is still unknown, but this motion can be critically altered by Cd^{2+} binding to an introduced cysteine at position 476. Cd^{2+} binding at this position prevents the gate from closing, either by interfering with its motion directly or by stabilizing the open state allosterically; in either case, this amino acid or its environment must change during gating. Because cysteines at 476 cannot be protected by the large pore-blocker TBuA, we suspect that this site may lie more peripherally, at least in the open state. Two intriguing possibilities are that it may lie on the moving part of the gate, or at a site of interaction between the voltage sensor and the gate.

Experimental Procedures

Mutagenesis and Expression

Cloned Shaker K^+ channels were transiently expressed in HEK293 cells, and we recorded from inside-out patches within 1–4 days after transfection. Methods for mutagenesis, transfection, identification of transfected cells, and rapid perfusion have all been described previously (Jurman et al., 1994; Holmgren et al., 1996a; Liu et al., 1996).

Mutants

For all experiments in this paper, we used a modified Shaker H4 "wild-type" channel, with mutations Δ6–46 (to remove N-type inactivation; Hoshi et al., 1990), T449V (to reduce C-type inactivation; López-Barneo et al., 1993), and C301S+C308S (to reduce the background sensitivity to MTS reagents; Holmgren et al., 1996a). These control "wild-type" channels showed approximately 10%–20% maximal current reduction with 1 mM intracellular MTSET.

The tandem dimers were prepared by subcloning into a construct prepared by Heginbotham and MacKinnon (1992). The A protomer contained the cysteine mutation and the B protomer was the "wild type" (as above).

Physiological Recording

Standard experimental solutions contained, in mM: 150 NaCl, 10 KCl, 3 $CaCl_2$, 1 $MgCl_2$, and 10 HEPES, at pH 7.4 (pipette); and 160 KCl, 0.5 $MgCl_2$, 1 EGTA, and 10 HEPES, at pH 7.4 (bath). Solutions with Cd^{2+} contained no EGTA.

Chemical Modification

MTS reagents (Toronto Research Chemicals, Downsview, Ontario) were made as stocks in water each day, held on ice, and mixed into the recording saline within a few minutes prior to use. 2,3-dimercapto−1-propanesulfonate (DMPS) was purchased from Aldrich.

For most mutants, modification rates were determined by measuring current reduction during a series of brief exposures to the MTS reagent. The current was plotted as a function of cumulative modification time and fit by a single exponential function (as in Figures 2B and 4B; also in Holmgren et al., 1996a; Liu et al., 1996). The MTS concentration was raised as high as 3 mM to measure the slowest rates, and lowered to 1 μM to measure the fastest rates. High MTS concentrations could also produce a rapid 10%–20% reduction in current that was also seen in wild type; this rapid phase was ignored in determining the specific modification rate.

For the mutants 483C and 486C, there was little or no reduction in current with MTSET treatment, so we measured the loss of sensitivity to Cd^{2+} blockade. For the 476C mutant, we did a single application of MTSET and measured the fraction of current with altered gating immediately after modification (results were like those in Figure 7B; only a single time point was obtained for each patch).

MTSEA experiments (on the 470C mutant) gave the same results in the presence of 20 mM cysteine on the opposite (extracellular) side of the membrane, indicating that this membrane-permeant reagent did not act from the extracellular side (Holmgren et al., 1996b). In addition, extracellular MTSEA (100 μM) had no effect on 470C channels in outside-out patches.

Analysis of Cd^{2+} Binding Models

For the three-state model diagrammed in the Discussion, we made a contour plot of the expected shift induced by Cd^{2+} as a function of the binding energy to each of the three states. At least one of the states must bind Cd^{2+} quite tightly (with a binding energy of approximately -10 kT) to explain the overall high affinity. The D $\rightleftharpoons$ A equilibrium constant, K(V), was an exponential function of voltage, and the A $\rightleftharpoons$ O equilibrium constant, L, was voltage-independent and constrained to the range 0.001–1000. Together these values were constrained to explain the g–V relation in the absence of Cd^{2+}. Using these parameters, we determined the sets of Cd^{2+} binding energies consistent with a shift of less than ± 10 mV. The possible solutions fall into the three classes described in the Discussion.

Acknowledgments

We thank Paula Smith, Stuart Forman and Keith Baker for helpful discussions. We also thank Bob Guy for prodding us into a serious treatment of multistate gating models. This work was supported by a National Institutes of Health research grant (to G. Y., NS 29693), an individual NIH NRSA (to Y. L.), and a Muscular Dystrophy Association postdoctoral fellowship (to M. H.).

Received May 14, 1997; revised June 5, 1997.

References

Aggarwal, S.K., and MacKinnon, R. (1996). Contribution of the S4 segment to gating charge in the *Shaker* K^+ channel. Neuron *16*, 1169–1177.

Akabas, M.H., Stauffer, D.A., Xu, M., and Karlin, A. (1992). Acetylcholine receptor channel structure probed in cysteine-substitution mutants. Science *258*, 307–310.

Armstrong, C.M. (1966). Time course of TEA^+-induced anomalous rectification in squid giant axons. J. Gen. Physiol. *50*, 491–503.

Armstrong, C.M. (1971). Interaction of tetraethylammonium ion derivatives with the potassium channels of giant axon. J. Gen. Physiol. *58*, 413–437.

Armstrong, C.M. (1975). Ionic pores, gates, and gating currents. Q. Rev. Biophys. *7*, 179–210.

Armstrong, C.M., and Hille, B. (1972). The inner quaternary ammonium ion receptor in potassium channels of the node of Ranvier. J. Gen. Physiol. *59*, 388–400.

Armstrong, C.M., Swenson, R.P., and Taylor, S.R. (1982). Block of squid axon channels by internally and externally applied barium ions. J. Gen. Physiol. *80*, 663–682.

Baukrowitz, T., and Yellen, G. (1996a). Use-dependent blockers and exit rate of the last ion from the multi-ion pore of a K^+ channel. Science *271*, 653–656.

Baukrowitz, T., and Yellen, G. (1996b). Two functionally distinct subsites for the binding of internal blockers to the pore of voltage-activated K^+ channels. Proc. Natl. Acad. Sci. USA *93*, 13357–13361.

Bezanilla, F., Perozo, E., and Stefani, E. (1994). Gating of *Shaker* K^+ channels: II. The components of gating currents and a model of channel activation. Biophys. J. *66*, 1011–1021.

Chervitz, S.A., and Falke, J.J. (1995). Lock on/off disulfides identify the transmembrane signaling helix of the aspartate receptor. J. Biol. Chem. *270*, 24043–24053.

Choi, K.L., Mossman, C., Aubé, J., and Yellen, G. (1993). The internal quaternary ammonium receptor site of *Shaker* potassium channels. Neuron *10*, 533–541.

Falke, J.J., Dernburg, A.F., Sternberg, D.A., Zalkin, N., Milligan, D.L., and Koshland, D.E., Jr. (1988). Structure of a bacterial sensory receptor. A site-directed sulfhydryl study. J. Biol. Chem. *263*, 14850–14858.

Fitzgerald, M.M., Musah, R.A., McRee, D.E., and Goodin, D.B. (1996). A ligand-gated, hinged loop rearrangement opens a channel to a buried artificial protein cavity. Nature Struct. Biol. *3*, 626–631.

French, R.J., and Shoukimas, J.J. (1981). Blockage of squid axon potassium conductance by internal tetra-N-alkylammonium ions of various sizes. Biophys. J. *34*, 271–291.

Grissmer, S., and Cahalan, M.D. (1989). Divalent ion trapping inside potassium channels of human T lymphocytes. J. Gen. Physiol. *93*, 609–630.

Hartmann, H.A., Kirsch, G.E., Drewe, J.A., Taglialatela, M., Joho, R.H., and Brown, A.M. (1991). Exchange of conduction pathways between two related K^+ channels. Science *251*, 942–944.

Heginbotham, L., and MacKinnon, R. (1992). The aromatic binding site for tetraethylammonium ion on potassium channels. Neuron *8*, 483–491.

Heginbotham, L., Lu, Z., Abramson, T., and MacKinnon, R. (1994). Mutations in the K^+ channel signature sequence. Biophys. J. *66*, 1061–1067.

Holmgren, M., Jurman, M.E., and Yellen, G. (1996a). Structure and function of the S4–S5 loop of the *Shaker* K^+ channel examined through cysteine mutagenesis and chemical modification. J. Gen. Physiol. *108*, 195–206.

Holmgren, M., Liu, Y., Xu, Y., and Yellen, G. (1996b). On the use of thiol-modifying agents to determine channel topology. Neuropharmacology *35*, 797–804.

Holmgren, M., Smith, P.L., and Yellen, G. (1997). Trapping of organic blockers by closing of voltage-dependent K^+ channels: evidence for a trap door mechanism of activation gating. J. Gen. Physiol. *109*, 527–535.

Hoshi, T., Zagotta, W.N., and Aldrich, R.W. (1990). Biophysical and molecular mechanisms of Shaker potassium channel inactivation. Science *250*, 533–538.

Joseph, D., Petsko, G.A., and Karplus, M. (1990). Anatomy of a conformational change: hinged "lid" motion of the triosephosphate isomerase loop. Science *249*, 1425–1428.

Jurman, M.E., Boland, L.M., Liu, Y., and Yellen, G. (1994). Visual identification of individual transfected cells for electrophysiology using antibody-coated beads. Biotechniques *17*, 876–881.

Larsson, H.P., Baker, O.S., Dhillon, D.S., and Isacoff, E.Y. (1996). Transmembrane movement of the *Shaker* K^+ channel S4. Neuron *16*, 387–397.

Liu, Y., Jurman, M.E., and Yellen, G. (1996). Dynamic rearrangement of the outer mouth of a K^+ channel during gating. Neuron *16*, 859–867.

Lopez, G.A., Jan, Y.N., and Jan, L.Y. (1994). Evidence that the S6 segment of the Shaker voltage-gated K^+ channel comprises part of the pore. Nature *367*, 179–182.

López-Barneo, J., Hoshi, T., Heinemann, S.H., and Aldrich, R.W. (1993). Effects of external cations and mutations in the pore region on C-type inactivation of Shaker potassium channels. Recept. Channels *1*, 61–71.

Loring, R.H., Dou, Y.M., Lane, W., Jones, G.S., and Stevenson, K.J. (1992). Aromatic trivalent arsenicals: covalent yet reversible reagents for the agonist binding site of nicotinic receptors. Mol. Brain Res. *15*, 113–120.

Loukin, S.H., Vaillant, B., Zhou, X.-L., Hoffman, R.J., Spalding, E.P., Kung, C., and Saimi, Y. (1997) Random mutagenesis reveals a region important for gating of the yeast K^+ channel, Ykc1. EMBO J., in press.

MacKinnon, R., and Yellen, G. (1990). Mutations affecting TEA blockade and ion permeation in voltage-activated K^+ channels. Science *250*, 276–279.

Miller, C., Latorre, R., and Reisin, I. (1987). Coupling of voltage-dependent gating and Ba^{++} block in the high-conductance, Ca^{++}-activated K^+ channel. J. Gen. Physiol. *90*, 427–449.

Sahin Toth, M., and Kaback, H.R. (1993). Cysteine scanning mutagenesis of putative transmembrane helices IX and X in the lactose permease of Escherichia coli. Protein Sci. *2*, 1024–1033.

Seoh, S.A., Sigg, D., Papazian, D.M., and Bezanilla, F. (1996). Voltage-sensing residues in the S2 and S4 segments of the *Shaker* K^+ channel. Neuron *16*, 1159–1167.

Shieh, C.-C. and Kirsch, G.E. (1994). Mutational analysis of ion conduction and drug binding sites in the inner mouth of voltage-gated K^+ channels. Biophys. J. *67*, 2316–2325.

Sigworth, F.J. (1994). Voltage gating of ion channels. Q. Rev. Biophys. *27*, 1–40.

Stauffer, D.A., and Karlin, A. (1994). Electrostatic potential of the acetylcholine binding sites in the nicotinic receptor probed by reactions of binding-site cysteines with charged methanethiosulfonates. Biochemistry *33*, 6840–6849.

Sun, Z.P., Akabas, M.H., Goulding, E.H., Karlin, A., and Siegelbaum, S.A. (1996). Exposure of residues in the cyclic nucleotide-gated channel pore: P region structure and function in gating. Neuron *16*, 141–149.

Taglialatela, M., Champagne, M.S., Drewe, J.A., and Brown, A.M. (1994). Comparison of H_5, S_6, and H_5–S_6 exchanges on pore properties of voltage-dependent K^+ channels. J. Biol. Chem. *269*, 13867–13873.

Tempel, B.L., Papazian, D.M., Schwarz, T.L., Jan, Y.N., and Jan, L.Y. (1987). Sequence of a probable potassium channel component encoded at Shaker locus of Drosophila. Science *237*, 770–775.

Yang, N., and Horn, R. (1995). Evidence for voltage-dependent S4 movement in sodium channels. Neuron *15*, 213–218.

Yang, N., George, A.L., Jr., and Horn, R. (1996). Molecular basis of charge movement in voltage-gated sodium channels. Neuron *16*, 113–122.

Yellen, G., Jurman, M.E., Abramson, T., and MacKinnon, R. (1991). Mutations affecting internal TEA blockade identify the probable pore forming region of a K^+ channel. Science *251*, 939–942.

Yellen, G., Sodickson, D., Chen, T.-Y., and Jurman, M.E. (1994). An engineered cysteine in the external mouth of a K^+ channel allows inactivation to be modulated by metal binding. Biophys. J. *66*, 1068–1075.

Yool, A.J., and Schwarz, T.L. (1991). Alteration of ionic selectivity of a K^+ channel by mutation of the H5 region. Nature *349*, 700–704.

Zagotta, W.N., Hoshi, T., and Aldrich, R.W. (1994). Shaker potassium channel gating. III: Evaluation of kinetic models for activation. J. Gen. Physiol. *103*, 321–362.